

## An insight into the origin of low-symmetry bridging phase and enhanced functionality in systems containing competing phases

Lingping Kong, Gang Liu, Wenge Yang, and Wenwu Cao

Citation: *Applied Physics Letters* **107**, 042901 (2015); doi: 10.1063/1.4927550

View online: <http://dx.doi.org/10.1063/1.4927550>

View Table of Contents: <http://scitation.aip.org/content/aip/journal/apl/107/4?ver=pdfcov>

Published by the AIP Publishing

### Articles you may be interested in

Near-field resonance shifts of ferroelectric barium titanate domains upon low-temperature phase transition  
*Appl. Phys. Lett.* **105**, 053109 (2014); 10.1063/1.4892364


Anisotropy of ferroelectric behavior of  $(1-x)\text{Bi}_{1/2}\text{Na}_{1/2}\text{TiO}_3-x\text{BaTiO}_3$  single crystals across the morphotropic phase boundary  
*J. Appl. Phys.* **116**, 044111 (2014); 10.1063/1.4891529

Phase transitions and electromechanical properties for barium titanate and lead titanate ferroelectric crystals under one-dimensional shock wave compression  
*J. Appl. Phys.* **112**, 114118 (2012); 10.1063/1.4768903


Monoclinic M C phase in (001) field cooled  $\text{BaTiO}_3$  single crystals  
*Appl. Phys. Lett.* **94**, 032901 (2009); 10.1063/1.3073716

Piezoelectric performances of lead-reduced  $(1-x)(\text{Bi}_{0.9}\text{La}_{0.1})(\text{Ga}_{0.05}\text{Fe}_{0.95})\text{O}_{3-x}(\text{Pb}_{0.9}\text{Ba}_{0.1})\text{TiO}_3$  crystalline solutions in the morphotropic phase boundary  
*J. Appl. Phys.* **96**, 6611 (2004); 10.1063/1.1810633


Frustrated by old technology?



Is your AFM dead and can't be repaired?



Sick of bad customer support?



**It is time to upgrade your AFM**

Minimum \$20,000 trade-in discount for purchases before August 31st

**Asylum Research is today's technology leader in AFM**

**OXFORD INSTRUMENTS**  
The Business of Science®

[dropmyoldAFM@oxinst.com](mailto:dropmyoldAFM@oxinst.com)

# An insight into the origin of low-symmetry bridging phase and enhanced functionality in systems containing competing phases

Lingping Kong,<sup>1,2</sup> Gang Liu,<sup>1,2,a)</sup> Wenge Yang,<sup>1,2</sup> and Wenwu Cao<sup>3,4,a)</sup>

<sup>1</sup>Center for High Pressure Science and Technology Advanced Research, Shanghai 201203, China

<sup>2</sup>High Pressure Synergetic Consortium, Geophysical Laboratory, Carnegie Institute of Washington, Argonne, Illinois 60439, USA

<sup>3</sup>Condensed Matter Science and Technology Institute, Harbin Institute of Technology, Harbin 150080, China

<sup>4</sup>Department of Mathematics and Materials Research Institute, The Pennsylvania State University, University Park, Pennsylvania 16802, USA

(Received 15 June 2015; accepted 17 July 2015; published online 27 July 2015)

High piezoelectric activity of ferroelectrics with morphotropic phase boundary (MPB) compositions has been the focus of numerous recent investigations. The concept of a bridging low-symmetry phase between competing phase structures of the MPB composition remains controversial due to the compositional inhomogeneity near the MPB and the lack of appropriate experimental techniques to delineate the complex crystal structures. We have studied a simple ferroelectric BaTiO<sub>3</sub> by employing a high resolution synchrotron-based technique, in which the formation of different symmetry regions due to chemical inhomogeneity can be ruled out. We observed two types of thermotropic phase boundaries, revealing the importance of interphase-strain in the formation of a bridging phase between competing phases and the enhancement of functionality. © 2015 AIP Publishing LLC. [<http://dx.doi.org/10.1063/1.4927550>]

Perovskite ferroelectrics are a fascinating class of materials for their excellent piezoelectric properties, which have been widely used in electromechanical devices (such as sensors, medical transducers, underwater sonars, and memory device), as well as for their rich physics underlying the high functional properties involving phase transitions.<sup>1–5</sup> For solid solution ferroelectrics with compositions in the vicinity of the morphotropic phase boundary (MPB), various functionalities, including piezoelectric activity, dielectric response, as well as energy dissipation, are significantly enhanced.<sup>5–7</sup> A remarkable advance made in searching for high piezoelectricity materials is the discovery of relaxor-PbTiO<sub>3</sub> (PT) single crystals with the MPB composition, such as Pb(Mn<sub>1/3</sub>Nb<sub>2/3</sub>)O<sub>3</sub>-PT (PMN-PT) and PbZn<sub>1/3</sub>Nb<sub>2/3</sub>O<sub>3</sub>-PT (PZN-PT) systems, in which piezoelectric coefficient  $d_{33}$  and electromechanical coupling factor  $k_{33}$  can reach as high as 2500 pC/N and 0.9, respectively.<sup>6</sup> At the MPB, phenomenological calculations predicted that the free energy profile of system is rather flat and an easy polarization rotation can be induced through a subtle monoclinic distortion of the lattice structure, which have also been experimentally demonstrated in various perovskite systems, including Pb(Zr,Ti)O<sub>3</sub> (PZT), PMN-PT, and PZN-PT.<sup>8,9</sup> A universal phase diagram for high-piezoelectric perovskite systems had been proposed based on the Landau theory,<sup>10</sup> with emphasized the importance of high-order expansion terms in the Landau free energy. Experiments demonstrated three types of monoclinic phases, i.e., M<sub>A</sub>, M<sub>B</sub>, and M<sub>C</sub> phases that can bridge competing higher symmetry phases, i.e., co-existing of rhombohedral (R), tetragonal (T), and/or orthorhombic (O) phases.

Those previous results suggested that a strong piezoelectric effect is associated with an intermediate low-symmetry

phase, which promotes an intriguing question: what is the physical role of the low-symmetry phase in the enhancement of functional properties near a phase boundary?

It is well known that for complex systems, such as relaxor-PbTiO<sub>3</sub>, chemical inhomogeneity and nano-polar regions are inevitable, adding to the confusion between local and average symmetries in structural investigations.<sup>11</sup> Most importantly, it is very difficult to conclusively identify low-symmetry phases at the MPB because the resolution of available facilities is not high enough to fully resolve the subtle difference in structures among all competing phases.<sup>12</sup> On the other hand, using a network of competing and coexisted domains, local monoclinic phase, symmetry lowering, and properties increasing phenomena have been observed by synchrotron-based techniques in pure BaTiO<sub>3</sub> at the O ↔ T thermotropic phase boundary (TPB),<sup>13–15</sup> which may be used as a simplified model of phase boundary in the MPB composition of solid solutions. In this study, synchrotron-based x-ray techniques with ultrahigh  $d$ -spacing resolution, together with Raman spectroscopy, were employed to accurately resolve the two types of TPBs in BaTiO<sub>3</sub>.

*In-situ* synchrotron XRD experiments were performed at the Argonne National Laboratory beam line 11-BM from 160 K to 320 K. The instrument resolution is  $\Delta d/d \sim 0.00017$ , representing the state-of-the-art  $d$ -spacing resolution for diffraction measurements.<sup>16</sup> Temperature dependent Raman spectroscopy measurements were performed using a 514.5 nm excitation laser source.

BaTiO<sub>3</sub> undergoes a series of ferroelectric phase transitions upon heating, from rhombohedral (R) to orthorhombic (O), then from O to tetragonal (T), and finally from T to the paraelectric cubic (C) phase.<sup>17–19</sup> Considering that the signature of a TPB is a thermal stabilized structure balancing between two or more competing phases,<sup>13,14</sup> it is possible to find TPBs around ferroelectric phase transition temperatures.

<sup>a)</sup> Authors to whom correspondence should be addressed. Electronic addresses: hit071202@gmail.com (Gang Liu) and dzk@psu.edu (Wenwu Cao).

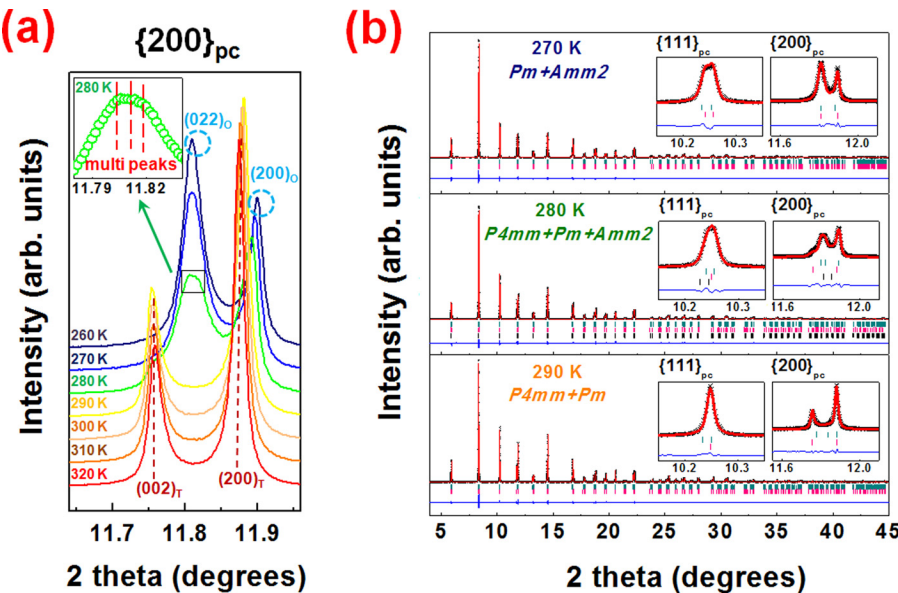


FIG. 1. Observation of TPB with a bridging phase: (a) High resolution synchrotron XRD profile for  $\{200\}_{pc}$  reflections of  $\text{BaTiO}_3$  from 260 K to 320 K. Inset: at 280 K, three resolved peaks in the diffraction angle range of  $11.79^\circ$ – $11.84^\circ$  are highlighted by red lines and (b) Rietveld refinements of the XRD pattern measured at 270 K, 280 K, and 290 K using  $Pm + Amm2$ ,  $P4mm + Pm + Amm2$ , and  $P4mm + Pm$  models, respectively.

To investigate the  $O \leftrightarrow T$  phase transition sequence, high resolution XRD patterns were collected from 260 K to 320 K and the diffraction profiles around pseudocubic  $\{200\}_{pc}$  diffraction peak were given in Fig. 1(a). At 280 K, multi-peak characteristic was observed within the diffraction angle range of  $11.79^\circ$ – $11.84^\circ$  (see the inset of Fig. 1(a)), indicating that the obtained XRD pattern cannot be satisfied by the single phase or mixed-phase models of the two competing phases, namely,  $Amm2$ ,  $P4mm$ , or  $Amm2 + P4mm$ , because the space group  $Amm2$  only allows for one  $\{200\}_{pc}$  peak and there is no peak corresponding to the space group  $P4mm$ . Therefore, there must be a low-symmetry phase contributing to the  $\{200\}_{pc}$  peak splitting, which can be further supported by crystallographic refinement results, as shown in Fig. 1(b). It was found that the  $Amm2$  structure persisted up to 260 K, above which monoclinic symmetry  $Pm$  began to emerge, associated with mixed-phase models of  $Pm + Amm2$ ,  $Pm + Amm2 + P4mm$ , and  $Pm + P4mm$  at 270 K, 280 K, and 290 K, respectively, then followed by a  $Pm \rightarrow P4mm$  phase transition above 320 K. This temperature-driven structural evolution demonstrated a thermodynamically stabilized structure among various competing phases over a broad temperature range ( $\sim 50$  K), agreeing well with the results of phase field modeling,<sup>14</sup> and confirmed the existence of TPBs with a bridging  $M_C$  phase. Furthermore, based on the results

shown in Fig. 1(b), detailed structural parameters as a function of temperature were obtained and listed in Table I, with emphasis on the mixed-phase and competing symmetry characteristics compared to the previous neutron results that only fitted to a single phase model.

To investigate another ferroelectric phase transition  $R \leftrightarrow O$ , XRD pattern from 180 K to 220 K was collected. Selected profiles at 200 K are shown in Fig. 2(a), in which one can see that peaks belong to both R and O were resolved clearly, revealing a mixed-phase phenomenon. Based on the refinement results as shown in Fig. 2(b), ferroelectric phase transition sequence of  $R3m \rightarrow R3m + Amm2 \rightarrow Amm2$  was concluded and the temperature dependent lattice parameters are listed in Table II. In contrast to the  $O \leftrightarrow T$  phase transition, there is no symmetry lowering intermediate phase between the R and O phases when crossing the phase boundary, which provides further support to the results of Raman spectroscopy shown in Fig. 2(c), in which no new peaks were observed.

Fig. 3(a) shows the  $\{200\}_{pc}$  Bragg reflections of  $\text{BaTiO}_3$  measured every 3 K throughout the temperature range of 160 K–211 K for both heating and cooling processes. One can see an obvious thermal hysteresis of  $\sim 20$  K by comparing heating and cooling processes in the same temperature range. Such a phenomenon means that  $R \leftrightarrow O$  phase

TABLE I. Structural parameters of  $\text{BaTiO}_3$  at the orthorhombic-tetragonal thermotropic phase boundary.

Temperature (K)	Orthorhombic (space group: $Amm2$ )		Monoclinic (space group: $Pm$ )		Tetragonal (space group: $P4mm$ )	
	Lattice parameters ( $\text{\AA}$ )	Phase (%)	Lattice parameters ( $\text{\AA}$ )	Phase (%)	Lattice parameters ( $\text{\AA}$ )	Phase (%)
270 <sup>a</sup>	$a = 3.9929$ ; $b = 5.6734$ ; $c = 5.6886$	42.2	$a = 4.0170$ ; $b = 3.9884$ ; $c = 4.0168$ ; $\beta = 90.125^\circ$	57.8	...	...
270 <sup>b</sup>	$a = 3.9874$ ; $b = 5.6751$ ; $c = 5.6901$	100	...	...	...	...
280 <sup>a</sup>	$a = 4.0038$ ; $b = 5.6748$ ; $c = 5.6892$	14.0	$a = 4.0218$ ; $b = 3.9904$ ; $c = 4.0142$ ; $\beta = 90.121^\circ$	60.1	$a = 3.9940$ ; $b = 4.0354$	25.9
280 <sup>b</sup>	...	...	...	...	$a = 3.9970$ ; $b = 4.0314$	100
290 <sup>a</sup>	...	...	$a = 4.0290$ ; $b = 3.9936$ ; $c = 4.0096$ ; $\beta = 90.117^\circ$	27.3	$a = 3.9941$ ; $b = 4.0365$	72.7
290 <sup>b</sup>	...	...	...	...	$a = 3.9925$ ; $b = 4.0365$	100

<sup>a</sup>This work.

<sup>b</sup>Data from Ref. 19.

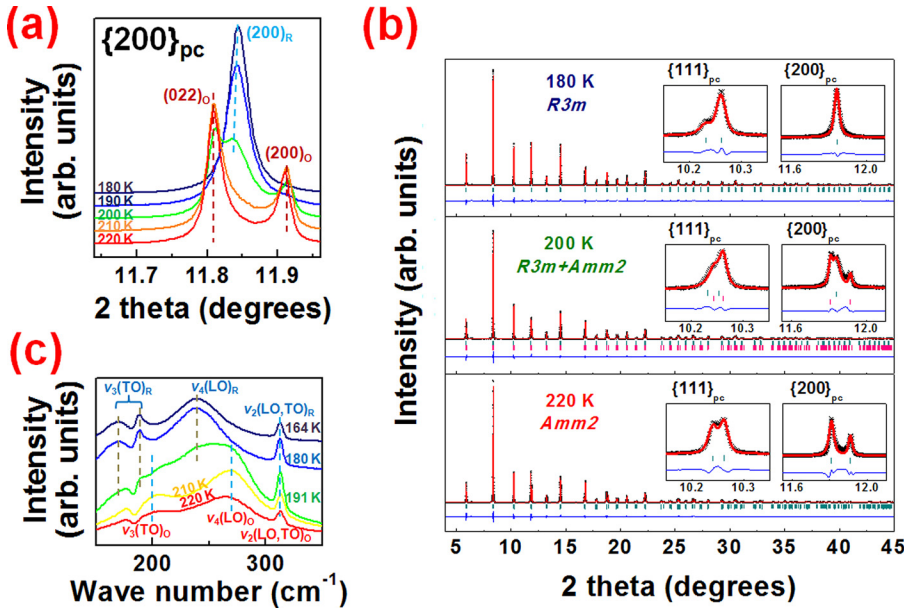


FIG. 2. Observation of TPB without a bridging phase: (a) High resolution synchrotron XRD profile for {200}<sub>pc</sub> reflections of BaTiO<sub>3</sub> from 180 K to 220 K; (b) Rietveld refinements of the XRD pattern measured at 180 K, 200 K, and 220 K using *R3m*, *R3m* + *Amm2*, and *Amm2* models, respectively; and (c) temperature-dependent Raman spectra from 164 K to 220 K. All vibration modes are well resolved and consistent with the results reported in Ref. 20.

transition in BaTiO<sub>3</sub> depends not only on temperature but also on the preceding thermal history, which can be understood from the fact that the initial developments of the O phase on heating and the R phase on cooling are hindered by the interphase-surface free energy and the strain to which the growing nuclei are subject to. Therefore, an additional thermal driving force is required to outweigh the surface, interface, and strain effects. In addition, it is well known that phonons are very sensitive to defects and interface/surface conditions.<sup>20</sup> Therefore, thermal barriers induced by the rich R/O interphase boundaries and/or particle surfaces could lead a difference in transition temperature among various parts of the whole system and also play an important role in thermal hysteresis. As shown in Figs. 3(a) and 3(b), although there is no symmetry lowering, the *R3m* + *Amm2* mixed-phase structure can be thermodynamically stabilized over a relative broad temperature range of ~20 K, demonstrating another type of TPBs without a bridging phase.

Ferroelectric phase transitions are believed to occur at an extremely short time-scale of 10<sup>-12</sup>–10<sup>-6</sup> s,<sup>21,22</sup> much faster than the heating or cooling speed in the present study, which is ~2 °C/min, indicating a time-independent behavior. However, a significant difference was found in measured {200}<sub>pc</sub> Bragg reflections between heating (II) and heating (III) (waiting for half hour after heating (II)) processes completed, as shown in Fig. 3(b), showing a time

dependent characteristic. Such an anomaly can be explained by the theory of phase transition kinetics, in which the rate of nucleation for the new phase, *r*, can be described as follows:

$$r \propto \exp\left(-\frac{\Delta F}{k_B T}\right), \quad (1)$$

where  $\Delta F$  is the energy barrier for the phase transition; and  $k_B$  and  $T$  denote the Boltzmann constant and temperature, respectively. Thus, the rate of nucleation will be delayed by increased energy barrier from additional interphase/surface energy and local strain fields, which has been observed in La-PZT systems.<sup>22</sup> Note that for heating (III) process, each Bragg reflection was collected half hour (~1800 s) after completing the respective test assigned to heating (II). Thus, as shown in Fig. 3(b), the slowing down in phase transition to 10<sup>3</sup> s time scale provides an opportunity to investigate the details on the kinetics and time-dependent properties in BaTiO<sub>3</sub>-based ferroelectrics. Based on the XRD refinement results, the O phase fractions for the four thermal processes, including heating, cooling, heating (II), and heating (III), are summarized in Fig. 3(c) with emphasis on the effects of thermal hysteresis and kinetic characteristics.

To explore the origin of the *M<sub>C</sub>* symmetry occurred at O-T TPBs and the absence of such a bridging phase at R-O

TABLE II. Structural parameters of BaTiO<sub>3</sub> at the rhombohedral-orthorhombic thermotropic phase boundary.

Temperature (K)	Rhombohedral (space group: <i>R3m</i> )		Orthorhombic (space group: <i>Amm2</i> )	
	Lattice parameters (Å)	Phase (%)	Lattice parameters (Å)	Phase (%)
180 <sup>a</sup>	$a = 4.0062$ ; $\alpha = 89.876^\circ$	100	...	...
180 <sup>b</sup>	$a = 4.0043$ ; $\alpha = 89.855^\circ$	100	...	...
190 <sup>b</sup>	...	...	$a = 3.9828$ ; $b = 5.6745$ ; $c = 5.6916$	100
200 <sup>a</sup>	$a = 4.0082$ ; $\alpha = 89.907^\circ$	50.6	$a = 3.9830$ ; $b = 5.6750$ ; $c = 5.6909$	49.4
210 <sup>b</sup>	...	...	$a = 3.9806$ ; $b = 5.6710$ ; $c = 5.6904$	100
220 <sup>a</sup>	...	...	$a = 3.9838$ ; $b = 5.6727$ ; $c = 5.6905$	100

<sup>a</sup>This work.

<sup>b</sup>Data from Ref. 19.



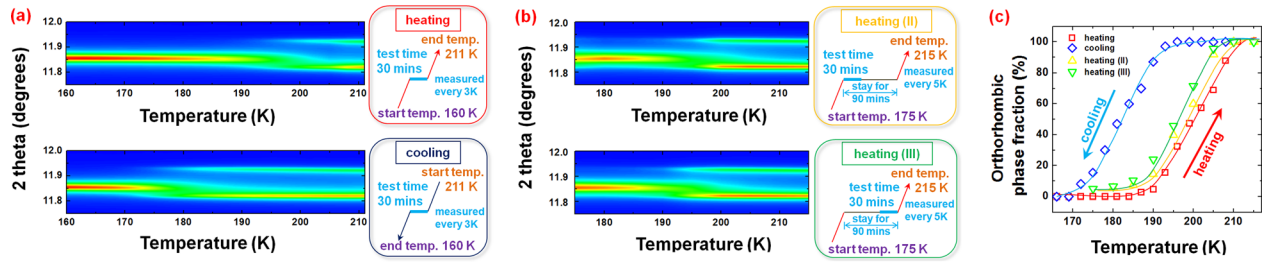


FIG. 3. Hysteresis and time dependent properties of  $R \leftrightarrow O$  TPB: (a) Collected  $\{200\}_{pc}$  reflections between 160 K and 211 K during heating and cooling processes; (b) collected  $\{200\}_{pc}$  reflections from 175 K to 215 K during heating (II) and heating (III) processes; and (c) temperature dependence of the O phase fractions for four thermal processes.

TPBs, the Gibbs free energy changes for  $R \rightarrow O$  and  $O \rightarrow T$  phase transitions can be expressed as follows:

$$\Delta G_{R \rightarrow O} = \Delta U_{R \rightarrow O} - T_{R \rightarrow O} \Delta S_{R \rightarrow O}, \quad (2)$$

and

$$\Delta G_{O \rightarrow T} = \Delta U_{O \rightarrow T} - T_{O \rightarrow T} \Delta S_{O \rightarrow T}. \quad (3)$$

Here,  $\Delta U$  and  $\Delta S$  denote the internal energy and entropy changes, respectively. Then, based on thermodynamic parameters (for  $R \rightarrow O$ :  $\Delta U = 196.74$  J/mol,  $\Delta S = 0.266$  J/mol·K, and  $T_{R \rightarrow O} = 200$  K; for  $O \rightarrow T$ :  $\Delta U = 422.41$  J/mol,  $\Delta S = 0.378$  J/mol·K, and  $T_{O \rightarrow T} = 280$  K),<sup>1,23</sup> changes of the Gibbs free energy for both ferroelectric phase transitions were calculated. It was found that  $\Delta G_{R \rightarrow O}$  ( $\sim 249.91$  J/mol) is much less than  $\Delta G_{O \rightarrow T}$  ( $\sim 528.25$  J/mol), indicating an easier phase transition process at a small energy cost for the  $R \rightarrow O$  phase transition, while for  $O \rightarrow T$  transition, the potential barrier between the two competing phases is relatively high, thus a bridging phase is thermodynamically necessary to flatten the energy profile.

The appearance of low symmetry bridging phase is also strongly associated with strain accommodation between the two competing phases.<sup>24</sup> Fig. 4(a) shows the unit cells of  $\text{BaTiO}_3$  in tetragonal, orthorhombic, and rhombohedral phases. One can see that if we treat every elementary cell as a parallelepiped, there are two types of planes for tetragonal (rectangle and square) and orthorhombic (rectangle and rhombus) phases, but only one type of rhombus plane for the rhombohedral phase. Thus, the coexistence of two phases forms four types of O/T interface but only two R/O interfaces, so that the corresponding lattice strain states can be qualitatively obtained, as illustrated in Figs. 4(b) and 4(c). Note that only the interface involving polarization rotation could induce symmetry lowering bridging phases. For all possible interfaces, only two types formed by rectangle and rhombus lattice planes satisfy such requirements, as depicted in Figs. 4(b4) and 4(c2). Considering the O/T interface shown in Fig. 4(b4), due to the large spontaneous strain  $c/a$  ( $\sim 1.01$ ) of the tetragonal phase, there must be an obvious difference between shear stresses along adjacent sides of rhombus lattice plane of orthorhombic cell, leading to

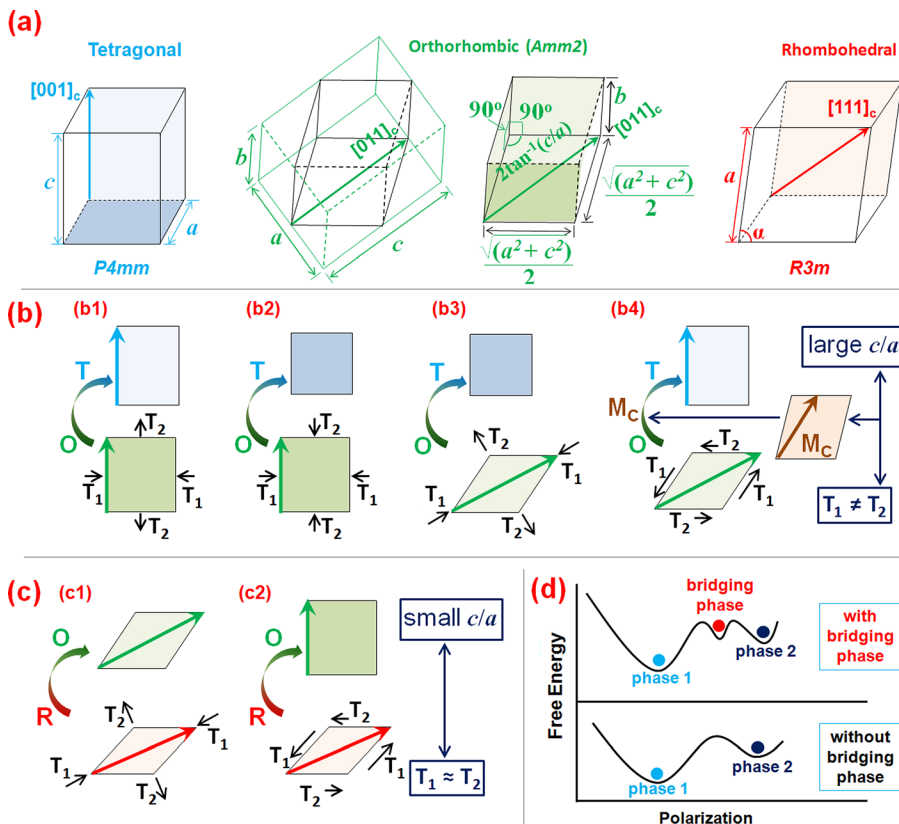


FIG. 4. Schematic of the formation of the bridging phase and its role in free energy profiles of a ferroelectric solid solution system: (a) Unit cells of  $\text{BaTiO}_3$  in tetragonal, orthorhombic, and rhombohedral phases. For tetragonal and orthorhombic phases, two distinct crystallographic planes in a parallelepiped elementary cell are differentiated by light and dark colors. The directions of spontaneous strain for all three ferroelectric phases are denoted by respective arrows; (b) and (c) all possible O/T and R/O interfaces; and (d) difference in free energy profile with and without the bridging phase. Please note that in (b) and (c),  $T_1$  and  $T_2$  denote the stresses applied on the elementary cells, while the rhombohedral, orthorhombic, and tetragonal phases are indicated by “R,” “O,” and “T,” respectively, and highlighted by red, green, and blue.

inhomogeneous transformations and an obvious difference in local strains for the two types of cells, giving rise to the low-symmetry distortion and a bridging phase at  $O \leftrightarrow T$  inter-phase boundaries. On the other hand, the spontaneous strain in the rectangle lattice plane of the orthorhombic unit cell is very small ( $\sim 1.003$ ), which means that the shear stresses along adjacent sides of a rhombohedral unit cell are almost the same so that nearly synchronous transformations occur, as shown in Fig. 4(c2). Thus, the spontaneous polarization in the phase transition can occur along a discontinuous path through a “jump” between potential wells. For this case, bridging phases are not necessary for the  $R \leftrightarrow O$  phase transition.

Based on the results of  $\text{BaTiO}_3$ , the dielectric response and piezoelectric activity were significantly improved as the system approaching both  $O \leftrightarrow T$  and  $R \leftrightarrow O$  TPBs, no matter if there is a bridging monoclinic phase, such as in the  $O \leftrightarrow T$  transition, or without a bridging phase, like the  $R \leftrightarrow O$  transition. In other words, an individual low-symmetry phase is not necessary for the enhanced properties. Moreover, ultrahigh piezoelectric activity ( $\sim 2300$  pC/N) was observed in PMN-0.31PT single crystals with R/M MPB composition, while much lower value of 1200 pC/N was found in PMN-0.34PT crystals with individual monoclinic structure.<sup>25</sup>

On the other hand, when the potential barrier between two competing phases is high, bridging phase may be generated to form complex phase boundaries. As illustrated in Fig. 4(d), these phase boundaries are strongly associated with the flattened energy profile by the introduction of a shallow potential well due to the addition of a bridging phase, thus enhanced properties are found in the vicinity with structurally less-stable characteristics.

In summary, by employing ultrahigh  $d$ -spacing resolution synchrotron-based technique, two types of TPBs in classic ferroelectrics  $\text{BaTiO}_3$  were experimentally demonstrated to have a general characteristic of the coexistence of competing phases over a broad temperature range. Our observations of the presence of a monoclinic phase at the  $O \leftrightarrow T$  transition and the absence of such a monoclinic phase at the  $R \leftrightarrow O$  phase strongly support the notion that structural uncertainty between competing phases is the key factor for the functional property enhancement behavior of ferroelectrics, while the presence of a bridging phase is not necessary. Generally speaking, in the vicinity of structural transitions, spontaneous polarizations and unit cell structures are less stable so that they can be easily altered by applying external fields, which cause the enhancement of various functional properties. This fundamental insight gained from our study

suggested that realizing a thermodynamically strong competing pair phases at the micro scale is critical to create enhanced functional properties in ferroic systems.

This work was supported by the National Key Basic Research Program of China under Grant No. 2013CB632900 and the NIH under Grant No. P41-EB2182. We specially thank Dr. Ho-kwang Mao for useful discussions. We appreciate Dr. Saul H. Lapidus and Dr. Matthew R. Suchomel for their help in the experimental procedure. The use of the Advanced Photon Source was supported by the U.S. Department of Energy, Office of Science, Office of Basic Energy Sciences, under Contract No. DE-AC02-06CH11357.

- <sup>1</sup>H. Fu and R. E. Cohen, *Nature* **403**, 281 (2000).
- <sup>2</sup>A. Toprak and O. Tigli, *Appl. Phys. Rev.* **1**, 031104 (2014).
- <sup>3</sup>A. Gruverman and A. Kholkin, *Rep. Prog. Phys.* **69**, 2443 (2006).
- <sup>4</sup>J. F. Scott, *Science* **315**, 954 (2007).
- <sup>5</sup>D. Damjanovic, *J. Am. Ceram. Soc.* **88**, 2663 (2005).
- <sup>6</sup>S. E. Park and T. R. Shrout, *J. Appl. Phys.* **82**, 1804 (1997).
- <sup>7</sup>G. Liu, S. J. Zhang, W. H. Jiang, and W. W. Cao, *Mater. Sci. Eng., R* **89**, 1 (2015).
- <sup>8</sup>B. Noheda, D. E. Cox, G. Shirane, J. A. Gonzalo, L. E. Cross, and S. E. Park, *Appl. Phys. Lett.* **74**, 2059 (1999).
- <sup>9</sup>B. Noheda, D. E. Cox, G. Shirane, J. Gao, and Z.-G. Ye, *Phys. Rev. B* **66**, 054104 (2002).
- <sup>10</sup>D. Vanderbilt and M. H. Cohen, *Phys. Rev. B* **63**, 094108 (2001).
- <sup>11</sup>B. Noheda, *Curr. Opin. Solid State Mater. Sci.* **6**, 27 (2002).
- <sup>12</sup>B. Noheda and D. E. Cox, *Phase Transitions* **79**, 5 (2006).
- <sup>13</sup>T. T. A. Lummen, Y. J. Gu, J. J. Wang, S. M. Lei, F. Xue, A. Kumar, A. T. Barnes, E. Barnes, S. Denev, A. Belianinov, M. Holt, A. N. Morozovska, S. V. Kalinin, L. Q. Chen, and V. Gopalan, *Nat. Commun.* **5**, 3172 (2014).
- <sup>14</sup>Y. J. Gu, F. Xue, S. M. Lei, T. T. A. Lummen, J. J. Wang, V. Gopalan, and L. Q. Chen, *Phys. Rev. B* **90**, 024104 (2014).
- <sup>15</sup>Ch. Eischenschmidt, H. T. Langhammer, R. Steinhausen, and G. Schmidt, *Ferroelectrics* **432**, 103 (2012).
- <sup>16</sup>P. L. Lee, D. Shu, M. Ramanathan, C. Preissner, J. Wang, M. A. Beno, R. B. Von Dreele, L. Ribaud, C. Kurtz, S. M. Antao, X. Jiao, and B. H. Toby, *J. Synchrotron Radiat.* **15**, 427 (2008).
- <sup>17</sup>W. J. Merz, *Phys. Rev.* **76**, 1221 (1949).
- <sup>18</sup>A. V. Hippel, *Rev. Mod. Phys.* **22**, 221 (1950).
- <sup>19</sup>G. H. Kwei, A. C. Lawson, S. J. L. Billinge, and S. W. Cheong, *J. Phys. Chem.* **97**, 2368 (1993).
- <sup>20</sup>E. T. Swartz and R. O. Pohl, *Rev. Mod. Phys.* **61**, 605 (1989).
- <sup>21</sup>A. Grigoriev, D. H. Do, D. M. Kim, C. B. Eom, B. Adams, E. M. Dufresne, and P. G. Evans, *Phys. Rev. Lett.* **96**, 187601 (2006).
- <sup>22</sup>Z. M. Sun, D. Z. Xue, H. J. Wu, Y. C. Ji, X. D. Ding, D. Wang, Y. D. Yang, and X. B. Ren, *Appl. Phys. Lett.* **102**, 222907 (2013).
- <sup>23</sup>Y. L. Li, L. E. Cross, and L. Q. Chen, *J. Appl. Phys.* **98**, 064101 (2005).
- <sup>24</sup>Y. Zhang, D. Z. Xue, H. J. Wu, X. D. Ding, T. Lookman, and X. B. Ren, *Acta Mater.* **71**, 176 (2014).
- <sup>25</sup>F. Li, S. J. Zhang, Z. Xu, X. Y. Wei, J. Luo, and T. R. Shrout, *J. Appl. Phys.* **108**, 034106 (2010).